Targeted metagenomics using probe capture detect a larger diversity of nitrogen and methane cycling genes in complex microbial communities than traditional metagenomics

H.M.P. Siljanen[1,2], L. Manoharan[2a], A.S. Hilts[2], A. Bagnoud[2b], R.J.E. Alves[2c], C.M. Jones[3], M. Kerou[2], F. L. Sousa[2], S. Hallin[3], C. Biasi[1,4], C. Schleper[2]

1. Department of Environmental and Biological Sciences, University of Eastern Finland, Kuopio, Finland
2. Department of Functional and Evolutionary Ecology, University of Vienna, Vienna, Austria
3. Department of Forest Mycology and Plant Pathology, Sweden University of Agricultural Sciences, Uppsala, Sweden.
4. Department of Ecology, University of Innsbruck, Innsbruck, 6020, Austria

Present address:

a. National Bioinformatics Infrastructure Sweden (NBIS), SciLifeLab, Department of Laboratory Medicine, Lund University, Lund, Sweden.
b. Membratec S, Ecoprac de Daval C 1, CH-3960 Sierre, Switzerland.
c. Climate and Ecosystem Sciences Division, Lawrence Berkeley National Laboratory, Berkeley, CA, USA

Corresponding authors:

Henri Siljanen, henri.siljanen@uef.fi

Christa Schleper, christa.schleper@univie.ac.at

Keywords: metagenomics, nitrogen cycling, methane cycling, probe hybridization targeted metagenomics, PCR amplicon sequencing, shotgun metagenomics

Manuscript contribution to the field

Metagenomic sequencing often yields limited numbers of sequences of rare microbial taxa or functional genes, preventing in-depth analyses of specific populations and functional groups. Amplicon-based approaches enable the higher diversity coverage of target populations, but the

drawback is the difficulty in designing unbiased primers that cover the highest intra-group diversity. Targeted metagenomics overcomes these challenges and results in similar community structure as traditional amplicon sequencing, while expanding the sequence space in a less biased metagenomic-based approach. Therefore, targeted metagenomics is an invaluable tool for studying the diversity of specific populations within complex natural microbiomes. Here, we present and evaluate a probe library designed for targeted metagenomics of nitrogen and methane cycling genes in complex communities.

Abstract

Microorganisms are key players in the global cycling of nitrogen (N) and carbon (C), controlling their availability and fluxes, including the emissions of the powerful greenhouse gases nitrous oxide (N_2O) and methane (CH_4). Characterizing the microbial functional guilds driving these processes is crucial for understanding ecosystem functioning and predicting their responses to environmental changes. Standard sequence-based characterization methods often reveal only a limited fraction of their diversity in nature because of their low relative abundance, the insufficient sequencing depth of traditional metagenomes of complex communities, and limitations in coverage of PCR-based assays. Here, we developed and tested a targeted metagenomics approach based on probe capture and hybridization to simultaneously characterize the diversity of multiple key metabolic genes involved in inorganic N and CH_4 cycling. We designed comprehensive probe libraries for each of the 14 target marker genes comprising 264,000 unique probes. These probes were used to selectively enrich the target genes in shotgun metagenomic libraries. In validation experiments with the mock communities of known microorganisms, targeted metagenomics yielded gene profiles similar to those of the original communities. Only GC content had a small effect on probe efficiency, as low GC targets were less efficiently detected than those with high GC, within the mock communities. Furthermore, the relative abundances of the marker genes obtained using targeted or traditional shotgun metagenomics from agricultural and wetland soils were significantly correlated, indicating that the targeted approach did not introduce significant quantitative bias. In addition, using archaeal *amoA* genes as a case-study, targeted metagenomics identified substantially higher taxonomic diversity and a larger number of sequence reads per sample, yielding diversity estimates 28 or 1.24 times higher than shotgun metagenomics or

amplicon sequencing, respectively. Notably, shotgun metagenomics detected only three out of the 84 *amoA* gene phylotypes detected using targeted metagenomics. Our results show that targeted metagenomics complements current approaches to characterize key microbial populations and functional guilds in biogeochemical cycles in different ecosystems, enabling more detailed, simultaneous characterization of multiple functional genes.

Introduction

The global nitrogen (N) and carbon (C) cycles are essential processes of the Earth's biosphere and crucial for ecosystem functioning (Zaehle 2013, Gruber and Galloway, 2008; Archer 2010; Falkowski et al., 2000; Steffen et al. 2015). All major N transformation processes (i.e., nitrogen fixation, nitrification, denitrification, dissimilatory nitrate reduction to ammonium (DNRA), and anaerobic ammonium oxidation, or anammox), are performed exclusively by the functional guilds of bacteria, archaea, and eukaryotes (Galloway et al., 2004; Stein and Klotz, 2016; Kuypers et al., 2018; Offre et al. 2013). Their activities regulate N availability for primary producers and microorganisms across ecosystems and control the production and consumption of the potent greenhouse gas nitrous oxide (N_2O) and other gaseous N compounds through processes such as nitrification, denitrification, and non-denitrifier N_2O reduction (Barnard, et al., 2005, Thompson et al., 2012; Jones et al., 2014; Prosser et al. 2020). Methane (CH_4) is another major product of the microbial trophic chain underlying C cycling, and, like the most inorganic N compounds, its production and consumption are also regulated by highly specific groups of microorganisms (Bodelier and Laanbroek 2004, Murrel and Jetten 2009, Conrad 2009). Importantly, CH_4 is the second most potent greenhouse gas after carbon dioxide (CO_2) and, together with N_2O, contributes at least 25% of the total global warming caused by greenhouse gases (Myhre et al., 2013; Friedlingstein et al., 2020; Lan et al., 2023).

Despite their important ecological role, microorganisms participating in inorganic N and CH_4 transformations typically constitute a small fraction of microbial communities in most soil, sediment, and aquatic ecosystems (Håvelsrud, et al., 2011; Palmer et al., 2012; Aanderud et al., 2015, Nelson et al, 2016, Ouygang and Norton 2020). Community profiling based on 16S rRNA

genes only allows for very limited information about microbial functions (Alteio et al. 2021). Even in the rare cases when functions can be inferred from organism phylogeny, the striking genetic and functional diversity within functional guilds remains concealed, such as that among their key metabolic enzymes (e.g., ammonia monooxygenase (*amoA*), Alves et al. 2018; methyl co-enzyme M reductase (*mcrA*), Borrel, 2019). Additionally, taxonomy-based approaches are inadequate in elucidating processes that have a broader taxonomic distribution than originally thought (e.g. Kuypers et al. 2018, Borrel 2019, Li et al. 2023; Saghaï et al., 2024). Shotgun metagenomics is the typical method of choice for obtaining a relatively unbiased picture of the natural microbiome, provided that issues with sample preparation, DNA extraction, library preparation, and sequencing method can be ruled out (Pan et al., 2010, Nnadozie, Lin and Govinden, 2015; Sinha et al., 2017; Sui et al., 2020). Nevertheless, in complex and diverse microbial communities such as those in soils and sediments, even deeply-sequenced metagenomes do not uncover the full diversity of microbial functional guilds and key functional genes owing to their typically low relative abundances within the broader community (Palmer et al., 2012, Orellana et al. 2019, Ouygang and Norton 2020, Zhao et al. 2023). As a low-cost alternative, the characterization of specific functional groups has long relied on the PCR amplification of genes that encode key metabolic enzymes, as for example, of organisms involved in various N and CH_4 cycling pathways (Knief 2015; Brauer et al. 2021; Alves et al. 2018; Romdhane et al. 2021, Clark et al. 2022). However, the gene diversity captured by gene-specific PCR assays is limited by the primers used, which introduce biases that make comparisons among different genes or samples difficult (Hallin and Lindgren, 1999; Throbäck al. 2004; Kolb et al., 2003; Siljanen et al., 2011). Furthermore, in complex microbial communities, target genes of interest are encoded by a large diversity of organisms, and usually include a large fraction of novel gene sequence variants from uncharacterized organisms (Jones et al. 2014; Saghaï et al 2023). Thus the geometric expansion of genomic data has made it increasingly obvious that designing a single PCR primer pair to target the inherent diversity of metabolic genes is highly problematic (Bonilla-Rosso et al. 2016). Therefore, linking ecosystem functions to microbial communities is often only possible through the complex and resource-intensive combinations of meta-omics and isotope labelling approaches (Tveit et al. 2015, Orellana et al. 2019).

126 Targeted high-throughput sequencing approaches, known as probe capture, also called
127 hybridization capture, hybridization-based target enrichment, or captured metagenomics, have
128 been used to study complex eukaryotic samples such as human exons, ancient human genomes,
129 plant transcriptomes, and cancer marker single nucleotide polymorphisms (Skoglund et al. 2014,
130 Ichida et al. 2019, Futema et al. 2012, Gasc et al., 2016, Kamil et al. 2021, Bewicke-Copley et al.
131 2019). A few studies have also used this approach to facilitate the in-depth study of microbial
132 communities using either 16S rRNA genes or other microbial functional genes (Denonfoux et al.,
133 2013; Manoharan et al. 2015, Noyes et al., 2017, Beaudry et al., 2021). The probe capture approach
134 relies on targeting specific short sequences within a broader genomic pool (e.g., full genomes,
135 genome or gene fragments) with biotin-labelled probes. The probes that hybridize with their target
136 regions are then selectively captured from the full genomic library using streptavidin-labelled
137 magnetic beads (Liu et al., 2016). Different from sequence capture, where multiple probes are
138 designed to cover a whole exon, captured metagenomics relies on the large databases of multiple
139 target genes clustered at predefined similarity cut-offs, which are used to design a large number of
140 generic probes that are able to capture an extended sequence space for each of these sequence
141 clusters (Kushwaha et al., 2015, Manoharan et al., 2015).
142
143 To improve detection and the characterization of important, but low abundant microbial guilds
144 involved in N and CH_4 cycling in natural communities, we developed and evaluated a probe-based
145 targeted metagenomics approach to key genes involved in these processes. In addition to the
146 enhanced resolution and coverage of genetic sequence space, this approach allows the parallel
147 analysis of distinct steps within N- and CH_4- cycling pathways, thus combining the advantages of
148 both shotgun metagenomics and amplicon-based approaches. Here, we present a new probe set for
149 targeting 14 distinct functional genes involved in inorganic N cycling (i.e., N fixation, nitrification,
150 denitrification, anammox, and DNRA), and three genes involved in CH_4 production and
151 consumption. We evaluated our approach using mock communities comprising of DNA from
152 microorganisms involved in inorganic N cycling, or CH_4 production or consumption with varying
153 gene GC% content, which is known to affect probe hybridization efficiency. As a proof-of-concept
154 for complex communities, we performed shotgun metagenomics and targeted metagenomics on
155 agricultural and wetland soil samples and compared the diversity of two functional markers, the

156 archaeal *amoA* genes (marker for ammonia oxidizers) and *nosZ* genes (marker for nitrous oxide
157 reduction).
158
159 **Materials and methods**
160
161 **Construction of the target gene databases (TDBs)**
162 Target gene databases (TDBs) were constructed, containing all identifiable variants for the
163 following key genes: the nitrogenase iron subunit (*nifH*), bacterial and archaeal ammonia
164 monooxygenase subunit A (*amoA)*, nitrite oxidoreductase beta subunit (*nxrB)*, hydrazine
165 oxidoreductase A (*hzoA)*, formate dependent nitrite reductase (*nrfA*), periplasmic nitrate reductase
166 alpha subunit (*napA*), respiratory nitrate reductase alpha subunit (*narG*), copper-containing nitrite
167 reductase (*nirK*), cytochrome cd_1 nitrite reductase (*nirS*), nitric oxide reductase subunit B (*norB*),
168 nitrous oxide reductase (*nosZ*), particulate methane monooxygenase subunit A (*pmoA*), soluble
169 methane monooxygenase component A alpha chain (*mmoX*), and methyl-coenzyme M reductase
170 I subunit alpha (*mcrA*).
171
172 Hidden Markov Model (HMM) models were generated in order to identify all variants of the target
173 genes from public databases (Fig. 1). These models were built based on reference sequence
174 alignments from curated databases already available for selected genes, such as *amoA* (Alves et
175 al., 2018), *pmoA* (Knief et al., 2015), *nosZ* (Jones et al., 2013), *nirK, nirS, nor* (Graf et al., 2014);
176 and the Fungene repository (Fish et al., 2013). For target genes where alignments were not
177 available, reference alignments were generated from gene sequence data publicly available on the
178 NCBI WGS-database, from the full length open-reading frame of each subunit, to cover all known
179 diversity in each gene. Structure-based searches of the Genbank nt- and envnt- database were
180 subsequently performed with nhmmer using the generated HMMs for every target gene (Wheeler
181 & Eddy, 2013) on a local supercomputer cluster (Centre of scientific computing CSC, Espoo,
182 Finland) (July 2017). The HMM models are available through Zenodo:
183 https://doi.org/10.5281/zenodo.15752134 (In script: probe-capture/2-
184 selected_outputs/hmmer_profiles.zip). This sequence search selection process generated ~600,000
185 unique sequences across all gene families. The obtained database was clustered to 100% identity
186 in order to remove duplicates sequences in database with cd-hit and manually inspected to exclude

187 16S rRNA genes. The final output comprised the target gene database (TDB; available through
188 Zenodo: https://doi.org/10.5281/zenodo.15752134 (In script: probe-capture/2-
189 selected_outputs/all_genes_compiled_ncbi_nt_envnt_fungene_split_file_0.fasta.gz (four files
190 ..file_0-3.fasta.gz)). The workflow can be seen in Fig 1. Scripts for Target gene database search
191 is available in Zenodo (/probe-capture/tree/main/3-
192 other_scripts/Henri_scripts/Script_probe_capture.sh).
193
194 **Generation of probes for target genes**
195 The MetCap bioinformatics pipeline was used as a protocol to produce probes from highly
196 complex datasets for targeted metagenomics (Kushwaha et al., 2015). Default parameters were
197 used for designing up to six unique 50mer probes for each sequence cluster in the TDBs (clustered
198 with an 80% identity clustering threshold), with melting temperature of 47 °C, resulting in a set of
199 263,111 unique gene-specific probes (Fig 1, and in Zenodo: probe-capture/2-
200 selected_outputs/Final_N_probes.list1.fasta). The probes were synthesized by NimbleGen SeqCap
201 EZ (Roche NimbleGen, Inc., Madison, USA) as Custom design (since the MetCap pipeline was
202 used for probe design, probe order was done with Roche HyperDesign tool:
203 www.hyperdesign.com), with biotin labelling to enable retrieval of the hybridized targets using
204 streptavidin coated magnetic beads (Kushwaha et al., 2015; Manoharan et al., 2015).
205
206 **Extraction of DNA from cultures and generation of mock community DNA samples**
207 DNA samples from mock communities encoding the genes of interest were generated by mixing
208 genomic DNA from different organisms in variable proportions, in order to simulate variation in
209 overall GC% content. The pool of DNA in the mock communities included DNA from:
210 *Nitrosospira multiformis*, *Nitrososphaera viennensis*, *Nitrospira defluvii*, Ca. *Kuenenia*
211 *stuttgartiensis* PCR fragment of the full-lenght *hzoA* gene, *Pseudomonas aeruginosa*, *Escherichia*
212 *coli*, *Shigella sonnei*, *Cupriavidus metallidurans*, *Cupriavidus necator*, *Dyadobacter fermentans*,
213 *Pseudomonas stutzeri*, *Rhodobacter sphaeroides*, *Salinibacter ruber*, *Sulfurimonas denitrificans*,
214 *Methylosinus trichosporium* Ob3b, *Methylocella tundrae*, *Methylomicrobium buryatense*,
215 *Methanoregula boonei*, and *Methanolacinia petrolearia*. Strain information, including genome or
216 fragment size and the number of target genes per organism are shown in Supplementary Table S1.
217 DNA from cultured organisms was extracted from 1% SDS-treated cell pellets in CTAB buffer,

218 followed by phenol:chloroform:isoamyl alcohol extraction and ethanol precipitation, as described
219 before (Jones et al., 2013). The relative abundances of the microorganisms in the mock
220 communities were multiplied with the median genome GC% contents to generate a weighted GC%
221 content of the pool of samples with the following values: 47, 50, 53, 57, 60, and 63 (Supplementary
222 Table S2). Pooling ratios of microorganisms' DNA were calculated based on the expected number
223 of functional genes in the extracted DNA, the DNA concentration (determined with a Qubit HS
224 dsDNA kit (Thermo)) and genome size. Relative gene abundances in mock communities were
225 calculated and compared to the sequences generated using targeted metagenomics. The relative
226 abundance of each gene was calculated against the sum of abundance values of all 14 genes in the
227 targeted metagenomes of the mock community samples (relative abundance of a specific gene =
228 100 x (gene reads / sum of reads of 14 genes)). The captured reads for mock community targeted
229 metagenomics are shown in Table S4.
230
231 **Annotation of coding sequences from the mock community dataset**
232 Predicted proteomes from the mock communities were retrieved from NCBI to count the number
233 of each functional genes per genome. For *Nitrospira defluvii*; NC_014355.1, genes were predicted
234 from the genome nucleotide sequence using Prodigal (v2.6.3) (Hyatt et al., 2010). Proteins were
235 annotated using KOFAM (HMM database of KEGG Orthologs (KO)). Each protein was assigned
236 the top hitting KO. Where available, cut-offs provided with KOFAMscan (Aramaki et al., 2020)
237 were used to filter spurious results.
238
239 **Extraction of DNA and determination of chemical parameters from environmental samples**
240 Samples from two different environments, an agricultural soil in Hungary (n = 3), and a wetland
241 in Bellefontaine, France (n = 3) (Table S3), were collected in order to assess the effectiveness of
242 the probe set in enriching functional genes in different sample contexts. Extraction of DNA from
243 the environmental samples was performed as previously described by Siljanen et al., (2019).
244 Briefly, samples were homogenized by bead-beating 0.5 g of soil at a speed of 5.5 m/s, for 30 sec
245 with phenol:chloroform:isoamyl alcohol extraction in CTAB buffer, followed by ethanol
246 precipitation. The quality of DNA extracts was assessed using a NanoDrop ND-1000 (Thermo),
247 and DNA concentration was measured with a Qubit HS dsDNA kit (Thermo). The soil chemical

248 parameters soil C/N ratio, pH, Fe II/III-, ammonium- and nitrate content were determined as
249 described earlier (Siljanen et al., 2019; Bagnoud et al, 2020).
250
251 **Targeted metagenomic library preparation, target enrichment of libraries and sequencing**
252 **with Illumina Miseq**
253 For each sample, sequencing indexes and sequencing adapters were provided as commercial
254 service by the Centre for Genomic Research (CGR) -laboratories, at the University of Liverpool,
255 Liverpool, UK. Libraries were produced with KAPA HyperPlus Library Preparation (Roche) kit
256 to produce insert sizes of 630 bp according to the manufacturer's instructions. The protocol is
257 shown in Fig. 1. and described here briefly: 150ng of environmental DNA was fragmented with
258 KAPA fragmentation buffer and KAPA Frag Enzyme at +37°C for 20min. Fragmented DNA was
259 ligated to SeqCap Adapters A and B, +20°C for 15 minutes. Fragments were purified 0.65x
260 volumes of AMPure XP Reagent for 5 min at room temperature in magnetic particle collector
261 (MPC). Then the clear supernatant was removed and the library was washed twice with 200 µl of
262 80% ethanol. The libraries were removed from MPC by eluting them to 53 µl of elution buffer (10
263 mM Tris-HCl, pH 8.0) by incubated two minutes. Each library was amplified for 7 cycles, with
264 KAPA HyperPlus Library Preparation kit in order to add the indexes for each sample (cycling
265 conditions: +98°C, 15 sec; 60° for 30 sec; +72°C for 30 sec). Amplified libraries were purified
266 with AMPure XP beads as above.
267 The hybridization reactions to the NimbleGen SeqCap EZ Developer Probe set were performed
268 according to the manufacturer's instructions. The hybridization was done in non-binding DNA
269 background 25 µg, on top of 1 µg of each library equally pooled Multiplexed DNA Sample Library
270 were added. The Multiplexed Hybridization Enhancing Oligo Pool (2,000 pmol in 2µl volume),
271 the SeqCap HE Universal Oligo (1,000 pmol in 1µl volume) and (1,000 pmol in 1µl volume)
272 SeqCap HE Index Oligo Pool) was mixed with 1 µg of equally pooled Multiplexed DNA Sample
273 Library. Two volumes of AMPure XP Reagent was added on top of the above mixture and
274 thoroughly mixed. Samples were incubated for 10 minutes to allow the sample library to bind to
275 the beads. Samples were placed on the MPC to capture the beads and the solution allowed to clear.
276 Once clear, the supernatant was discarded carefully, to not disturb the beads. Afterwards 190 µl of
277 80% ethanol was added to the samples containing the bead-bound DNA samples. The samples
278 were left on the MPC during this step. Samples were incubated at room temperature for >30

279 seconds. The 80% ethanol was carefully removed and discarded, without disturbing the beads.
280 Beads were dried at room temperature with the tube lid open for 5 minutes (or until dry).
281 A master mix of the following reagents was prepared, scaling up to reflect the number of captures:
282 7.5 µl of the 2x Hybridization Buffer, 3 µl of Hybridization Component A. Then 10.5 µL of the
283 Hybridization Buffer/Hybridization Component A mix from the previous step was added to the
284 bead-bound DNA sample. Samples were removed from the MPC and mixed thoroughly. It was
285 important that enough mixing was performed at this step to yield a homogeneous mixture. It was
286 left to sit at room temperature for 2 minutes. Sampled were then placed on the MPC. After liquid
287 cleared, 10.5 µL of supernatant (entire volume) was removed and placed in a new tube containing
288 4.5 µl of the SeqCap EZ Developer Probe pool. This was mixed thoroughly. Hybridization
289 incubation was performed in a thermocycler using the following program with heated lid set to 10
290 °C above the block temperature: incubation was 95°C for 5min, and 47°C for 72 hours (SeqCap
291 EZ HyperCap Workflow protocol, Manoharan et al., 2015).
292 To purify the hybridized libraries the SeqCap Pure Capture Bead Kit was used. To prepare the
293 beads for binding the samples, 50 µl of beads (streptavidin coated magnetic beads) was added to
294 the 1.5 ml tube at room temperature for capturing reaction. Tubes were placed on a MPC, the
295 supernatant removed and beads were washed two times with 100 µl of 1x Bead Wash Buffer.
296 Afterwards it was removed from the MPC and mixed by pipetting up and down. Beads were bound
297 on the magnetic particle collector. Once the liquid was clear, the supernatant was removed. In the
298 second wash, the beads were aliquoted with 50 µl of 1X Bead Washing Buffer. Beads were bound
299 and the supernatant again removed. One hybridization sample (15 µl volume) was added to the
300 washed SeqCap Pure Capture Beads. Samples were bound to the beads by placing the samples in
301 a thermocycler at +47°C for 15 minutes (heated lid at +57°C). Then 100 µl of 1x Wash Buffer was
302 added on top of the Capture Beads and bead-bound DNA and mixed thoroughly. The tube was
303 placed on the MPC to capture the beads. The solution was allowed to clear, and the supernatant
304 removed, while being careful not to disturb the beads. Afterwards, 200 µl of 1x Stringent Wash
305 Buffer was added to each capture reaction. Those were mixed by pipetting up and down, when
306 tubes were not in a MPC. Samples were placed in the thermocycler to +47°C for 5 minutes. The
307 wash was repeated with 1x Stringent Wash Buffer. Next, 200 µl of 1x Wash Buffer I was added,
308 vortexed for 10 second, and incubated 1 minute at room temperature. Once the solution was clear,

309 it was removed, again being careful not to disturb the beads. The washing with 1X Wash buffer II
310 was repeated, and then 1x with Washing Buffer III. Samples were removed from the MPC and 53
311 µl of PCR-grade water was added to the bead-bound sample. Sampled were then incubated at room
312 temperature for 2 minutes and placed in the MPC. Then 50 µl of clear solution was collected in a
313 new tube.
314
315 Sequencing for probe hybridized and washed DNA was performed with Illumina MiSeq PE300
316 chemistry in the Centre for Genomic Research (CGR), University of Liverpool, Liverpool, UK,
317 resulting in 198,700-311,500 reads per sample for the environmental samples and up to 2,600,000
318 reads for the mock communities.
319
320 **Targeted metagenomics read processing and mapping**
321 All six possible reading frames of the nucleotide sequence reads generated by the targeted
322 metagenomic sequencing of the mock community samples were translated using transeq from the
323 EMBOSS package (v6.6.0.0) (Rice et al., 2000). These were mapped to the genomes using
324 DIAMOND blastp (v2.0.6.144) (Buchfink et al., 2015), with a minimum percentage identity of
325 60%. This threshold was selected as it resulted in the largest percentage of mapped reads while
326 being stringent enough to prevent spurious mappings. No minimum coverage was used to account
327 for reads that did not fully overlap with the proteins from the mock community dataset. For each
328 direction, up to four matches were retained, to account for cases where a single read spanned
329 neighboring proteins. Multiple matches in the same direction could overlap by up to 15 amino
330 acids to account for possible protein fusions or sequencing errors. The blastx searches against the
331 *refseq* database (Altschul et al., 1990) were performed in order to remove duplicates or reannotate
332 falsely annotated entries due to the presence of homologous gene families in our dataset (*amoA*
333 vs. *pmoA*, *nxrB* vs. *narH* nitrate reductase or *napA*+*narG* vs. *nrfA*). The blastx search was done to
334 evaluate whether the read was correct or not, and the run was made with the default parameters of
335 blast. Each of the (up to four) matches were used to assign KOs to the reads, based on the predicted
336 KOs of the proteins to which they mapped. If, in a given direction, a read was assigned the same
337 KO multiple times, this was collapsed into a single hit, retaining the hit with the best E-value.
338
339 **Evaluation of functional annotation of reads**

340 Protein predictions for each read were performed using nhmmer from the HMMER suite
341 (v.3.3)(Eddy 2011) using the in-house generated HMMs for target genes as well as KOFAM as
342 described above. An inclusion threshold of <0.0001 was used when assigning protein predictions
343 for the reads. For a given read, using all six of the translated frames, up to four protein assignments
344 could be made, evaluated based on KO bit scores or identity filtering. Reads assigned KOs for the
345 function of interest were counted as positively identified hits. Subsequently, reads were mapped
346 to their corresponding coding sequences (CDS) from the mock community organisms to determine
347 which reads constituted "true positives" (TP) or "true negatives" (TN). Reads mapped to a given
348 CDS were assigned functions according to the above-mentioned KOFAM CDS annotation as their
349 "true function". If the HMM assignment (both in-house and from KOFAM) of a read matched the
350 functional assignment of the CDS to which it was mapped, then it was counted as a TP. The TP,
351 false positive (FP), and false negative (FN) values were summed up for all models using all
352 methods, and precision and recall were calculated. Read mapping (described above) was used to
353 determine the total number of possible TPs of the reads (Fig. S6), from which the actual number
354 of TPs was subtracted to calculate the number of FNs. Precision was calculated as the ratio of TPs
355 to total positive detections (i.e., number of TPs and FPs). Recall was calculated as the ratio of TPs
356 to all theoretically obtainable true positives (i.e., sum of TPs and FNs). The script is available on
357 Zenodo: https://doi.org/10.5281/zenodo.15752134 (/probe-capture/tree/main/3-
358 other_scripts/Angus_scripts).
359
360 **Shotgun metagenomics library preparation, sequencing with Illumina HiSeq and analysis**
361 Shotgun metagenomic sequencing was performed on environmental DNA (n = 3) from agricultural
362 soil and wetland soil (Table S3), extracted as described above for TDB production. Illumina
363 TruSeq library preparation with an insert size of 250bp was carried out with 1 μg of DNA and
364 sequencing was performed in Illumina HiSeq PE150 lane as a commercial service in Vienna
365 Biocenter Core Facility (VBCF, Austria) and Microsynth AG, Switzerland. In this approach, the
366 previously generated HMM profiles were used to identify the target gene pools (E < 0.001). The
367 predicted functions of each identified sequence were confirmed by tblastx against the *refseq*
368 database, using DIAMOND (Buchfink et al., 2015). Annotation and identity information was
369 further processed with awk in unix and in Rversion 3.5.3 to produce lists of community structures
370 for each target gene. The relative abundance of each gene was normalized against the sum of total

371 reads, Table S4: Relative abundance of gene x = (Abundance of gene x / total reads sequenced) x
372 100.
373
374 **_amoA_ gene amplicon sequencing**
375 Archaeal *amoA* gene amplicons from environmental DNA (n = 3) from the agricultural soil were
376 generated as described earlier by Siljanen et al., (2019), and sequencing was performed with
377 Illumina MiSeq PE250, in LGC, Münich, Germany. In brief, *amoA* gene amplicons were generated
378 using 0.6 ng DNA template with GoTaq DNA polymerase (Promega) and 0.5 µM primers
379 (CamoA_19F [5'-ATGGTCTGGYTWAGACG-3'] and TamoA_632R-4 [5'-
380 GCKGCCATCCATCKRTANGTCCA-3']) with a 5'-prime Illumina sequencing adaptor [5'-
381 CTCTTTCCCTACACGACGCTCTTCCGATCT-3'] for both end of above primers for making
382 the indexing possible in the sequencing service laboratory. Cycling conditions were the following:
383 1min initial denaturation at 95°C, 30sec denaturation at 94°C, 30sec annealing at 60°C and 45sec
384 extension at 72°C, with 35 cycles. PCR reactions were performed in triplicate for each sample (n
385 = 3), and purified with the High Pure PCR product purification kit (Roche). Sequencing indexes
386 were added by LGC, where libraries were equally pooled and sequenced with Illumina MiSeq
387 PE250.
388
389 **Processing of amplicon _amoA_ reads**
390 Archaeal *amoA* (Thaumarchaeal-*amoA*, *TamoA*) amplicon reads processing was carried out by a
391 custom-based Python script available at Zenodo: https://doi.org/10.5281/zenodo.15752134; /probe-
392 capture/tree/main/1-scripts/1-amplicon_seq_script_v1.sh -folder). Briefly, quality trimming of
393 sequencing reads was performed by truncating amplicon forward read R1 reads to 200bp and
394 reverse read R2 180bp, discarding all reads with an expected error greater than 0.5. The *amoA*
395 reads were dereplicated and amplicon sequence variants (ASVs) were assigned to taxonomic bins
396 described in the reference *amoA* gene database (Alves et al. 2018) using a 55% identity cutoff with
397 USEARCH8 (Edgar, 2010). Chimeras were filtered out with UCHIME (Edgar, 2011). For the
398 remaining ASVs, quality controlled R1 and R2 reads were fused together, classified with UCLUST
399 in QIIME (Caparaso et al., 2010) and clustered to OTUs with 97% sequence identity cut-off for
400 each taxonomic bins. Taxonomic bins of each *TamoA* gene cluster were generated using the
401 reference gene database and taxonomy by Alves et al. (2018) (Altschul et al. 1990; Callahan et al.,

402 2016). Relative abundance of *TamoA* taxonomic bins was calculated as follows: Relative
403 abundance of *TamoA* taxonomic bin x = (Abundance of *TamoA* taxonomix bin x / total *TamoA*
404 reads) x 100. In Fig. 4A, the relative abundance of each taxonomic bin (relative to the column
405 sum) was plotted for each sample. The sequencing depth for the *TamoA* gene amplicon library was
406 ~27,000-58,000 PE250 reads per sample up to 31Mb for the agricultural soil (Table S4).
407
408 **Processing of metagenomic *amoA* reads**
409 Archaeal *amoA* (Thaumarchaeal-*amoA*, *TamoA*) reads from targeted- and shotgun metagenomics,
410 were identified with the *TamoA* in-house HMM model. The forward reads were dereplicated and
411 assigned to the reference *amoA* gene database using a 55% identity cutoff with USEARCH8
412 (Edgar 2010). Chimeras were filtered out with UCHIME (Edgar 2011), all reads were clustered
413 with UCLUST with 97% sequence identity in QIIME and assigned to taxonomic bins based on the
414 closest *amoA* genes from the taxonomy database of OTUs (Alves et al. 2018) (Caporaso 2010).
415 Relative abundance was calculated as follows: Relative abundance of *TamoA* taxonomic bin x =
416 (Abundance of *TamoA* taxonomix bin x / total *TamoA* reads) x 100. In the targeted metagenomics
417 approach, multiple detection of the same taxonomic bin is possible because of six probes are used
418 for each sequence cluster. However, when relative abundance for each detected taxonomic bin is
419 calculated for targeted metagenomic, if multiple detection occurs in the relative abundance
420 calculation the community composition is balanced because of equal number of probes per each
421 sequence cluster. Therefore, the relative abundance of different sequencing methods can be
422 compared. The sequencing depth for the *TamoA* gene for three shotgun metagenomics *TamoA*
423 reads out of ~22-58M PE150 reads per sample up to 17 Gb, and for targeted metagenomics 4472-
424 8230 *TamoA* reads out of ~220-311k PE300 reads per sample up to 160 Mb, for the agricultural
425 soil (Table S4). The metagenomic reads processing is described in the custom-made script
426 available at Zenodo: https://doi.org/10.5281/zenodo.15752134 (targeted with probe-capture:
427 tree/main/1-scripts/2-probe_capture_script_v1.sh, and shotgun metagenomics: tree/main/1-
428 scripts/3-metagenomics_script_v1.sh).
429
430 **Phylogenetic placement analysis of *nosZ* reads from shotgun and targeted metagenomics**
431 **libraries.**

432 A reference alignment and phylogeny for *nosZ* was generated from full length *nosZ* amino acid
433 sequences obtained from genomes downloaded from the NCBI genome database (accessed
434 October 2019). A profile HMM for *nosZ* was generated from a previously published *nosZ* dataset,
435 as described above (Graf et al, 2022). Reads were converted to amino acid sequences and then
436 aligned using *hmmalign* within the HMMer suite (v.3.1.2)(Eddy 2011), and the homologous
437 sections were identified using FastTree (v. 2.1.11, Price et al., 2010). The reference protein
438 alignment was used for phylogenetic reconstruction using IQ-TREE (v1.6.12) with best model
439 selection and 1000 ultrafast bootstraps. The Le-Gascuel (LG) substitution model with 10 rate
440 categories was selected after automatic model selection. For the phylogenetic placement of *nosZ*
441 reads obtained using either shotgun metagenome sequencing (n=3) or targeted metagenomics
442 (n=3) of the agricultural site, the relevant reads were pooled together and clustered with CD-HIT
443 (Fu et al., 2012) at 90% sequence identity before translating and aligning to the reference *nosZ*
444 alignment using *hmmalign*. The translated reads were then placed in the reference phylogeny using
445 the next generation evolutionary placement algorithm (EPA-NG v0.3.8; Barbera et al., 2019), with
446 the same model parameters as used for constructing the reference phylogeny. The placement
447 positions with the highest likelihood weight ratio were plotted on the reference phylogeny in R
448 using the 'ggtree' package (v3.4.2, Yu et al., 2016). Script available for nosZ phylogenetic
449 placements at Zenodo: https://doi.org/10.5281/zenodo.15752134 (/probe-capture/tree/main/3-
450 other_scripts/Chris_Jones_scripts).
451
452 **Data and script availability**
453 The shotgun metagenomic, targeted metagenomic and *amoA* amplicon sequencing data have been
454 deposited in NCBI SRA under the Bioproject numbers PRJNA898102 and PRJNA488558. All
455 scripts are available at Zenodo: https://doi.org/10.5281/zenodo.15752134 . The repository contains
456 as well the target gene database (probe-capture/2-
457 selected_outputs/all_genes_compiled_ncbi_nt_envnt_fungene_split_file_0.fasta.gz (four files
458 ..file_0-3.fasta.gz), and the final probe sequences (probe-capture/2-
459 selected_outputs/Final_N_probes.list1.fasta).
460
461
462 **Results**

463

464 **Benchmarking gene detection and quantification using targeted metagenomics in mock**
465 **communities**

466 The targeted metagenomic approach was evaluated using mock microbial communities comprising
467 predefined mixtures of genomic DNA from 14 bacterial and three archaeal strains, together
468 containing all 14 functional genes targeted by the probes and mixed in different proportions to
469 produce six different median G+C contents ranging from 47% to 62% (Table S1). The overall
470 relative abundances of target genes in the captured metagenomes across all GC% categories were
471 correlated with their abundance in the original mock communities ($r = 0.78$ ($P < 0.0001$) (Fig. 2).
472 Comparisons between the relative abundance of individual genes in the mock communities as
473 compared to captured metagenomes revealed highly similar values (t = 1.8518e-10, df = 174.83,
474 $P > 0.05$), with the exception of the *nirK* and the *hzoA* genes (Fig. S1a,b). Pearson correlation
475 coefficients across all GC% categories varied between 0.76 and 0.93, although correlations were
476 stronger within higher GC% categories (57%-63%; R = 0.80-0.93) than within lower GC%
477 categories (47%-53%; R = 0.76-0.79) (Fig. S1). The probe capture targeted metagenomics
478 produced 61-72% of target gene sequences from the total sequenced library of the mock-
479 communities (Table S4).

480

481 **Precision of gene identification in mock communities**

482 Precision for the in-house HMMs ranged from 74.1% (*nifH*) to 100% (*mcrA*) (Fig. S5). The
483 average precision of the models was 93.4%, with a median of 99.8% (excluding *amoA* and *pmoA*).
484 The recall ranged from 42.8% (*nxrB*) to 100% (*mcrA*). The average recall was 81.9%, with a
485 median recall of 82.8%. Because KEGG only provides a single model covering the homologous
486 genes *pmoA* and *amoA*, it was not possible to accurately calculate the precision and recall for these
487 genes individually. A precision estimate could still be determined for the two genes, where a "true
488 positive" is defined as a hit for a read identified by the in-house models as *amoA* or *pmoA* mapped
489 to a CDS identified by the HMM for (*a*/*p*)*moA* genes provided by KEGG (K10944). In this case,
490 the precision values for the *amoA* and *pmoA* genes were estimated to be 96.9%, and 100%,
491 respectively. It is important to note that these estimates do not exclude the possibility that the in-
492 house models misclassified reads belonging to these homologous protein families.

493

494 Precision and recall values were similar using KOFAMs instead of in-house HMMs. However, the
495 results for *amoA* and *pmoA* genes were combined due to a single model for the associated KO for
496 both genes, as mentioned above. Precision ranged from 76.5% (*amoA*/*pmoA*) to 100.0% (*mcrA*),
497 while recall varied from 34.3% (*nifH*) to 100% (*mcrA* and *nxrB*). The average and median
498 precision values were 94.5% and 97.7%, while the average and median recall values were 93.39%
499 and 99.03%, respectively. The precision of KOs was lower for *napA* than for other genes when
500 compared with custom DNA HMMs. This could be accounted for by the presence of formate
501 dehydrogenase, a known homolog of *napA*. Formate dehydrogenase (K00123) was indeed
502 identified among the genomes used for the mock community, so it is possible that the custom
503 HMM was misclassifying reads originating from this known ortholog to *napA* (Cerqueira et al.,
504 2015).
505
506 **Higher number of reads for all target functional genes but similar relative abundance**
507 **obtained with targeted compared to shotgun metagenomics from complex environmental**
508 **samples**
509 We investigated the efficiency of the targeted metagenomics approach in natural complex
510 ecosystems by directly comparing this approach with shotgun untargeted metagenomics generated
511 with a nearly 100 times higher amount of sequencing (~66 Mb and ~6.4 Gb per sample,
512 respectively) from wetland soils in Bellefontaine, France, and from an agricultural field in Hungary
513 (Table S4). These soils represent distinct ecosystems with average physicochemical conditions,
514 such as water content and oxygen concentration, and N availability that favors different
515 distributions of functional genes (Jones et al. 2014). Despite the large difference in sequencing
516 depth, targeted metagenomics generated a much larger set of target functional genes (Fig. 3). In
517 both the agricultural and wetland site the targeted metagenomics approach detected 14 out of 15
518 gene-clusters and the shotgun approach 13 out of 15 genes (*mcrA* was not detected in the
519 agricultural site and *hzoA* not in the wetland site). Moreover, up to 60 times as many identified
520 gene sequences were detected using the probe capture compared to shotgun metagenomics (Fig.
521 3, Table S4). The relative abundances of functional genes in captured metagenomes correlated
522 significantly with that in shotgun metagenomes from both the agricultural field (R_{Pearson} = 0.96,
523 d.f.=14, $P < 0.00001$) and the wetland (R_{Pearson} = 0.70, d.f,=14, $P < 0.01$). The relative abundances
524 of target genes were different between the two approaches ($P > 0.00001$) (Fig. 3). Moreover,

525 increased relative abundance was detected with targeted compared to shotgun metagenomics in
526 the agricultural site for *nifH*, *TamoA*, *nrfA*, *napA*, *nirK*, *nirS*, *norB*, *nosZ* and *mmoX* (Fig. 3a) genes
527 and the wetland site for *nifH*, *napA, narG* and *nirS* (Fig. 3b) genes. The targeted approach
528 generated a much higher number of reads for all target genes in both sites than shotgun
529 metagenomics (Target reads in Table S4).
530
531 The different relative abundances of functional genes in the two ecosystems reflected known
532 differences in their environmental conditions: (i) N_2 fixation genes were expectedly higher in the
533 unfertilized wetland; (ii) Genes involved in ammonia oxidation and nitric and nitrous oxide
534 reduction were higher in the agricultural soil, which is likely to be more oxic and also subject to
535 N fertilization which increase inorganic N cycling; (iii) Genes involved in methanogenesis were
536 more abundant in the wetland, where anoxic conditions and methane production typically occur.
537
538 **Comparing diversity recovered for specific target genes from amplicon, targeted and**
539 **shotgun metagenomics from complex environmental samples**
540 In order to compare the diversity of specific functional genes detected by targeted metagenomics,
541 shotgun metagenomics and PCR amplicon sequencing we focused on the archaeal *amoA* gene as
542 a test case, as it is the second most sequenced gene in NCBI indicative of its ecological importance,
543 and for which there is a comprehensive reference database for classification available (Alves et
544 al., 2018). Moreover, archaeal ammonia oxidizers (AOA) typically outnumber their bacterial
545 counterparts in most environments (Leininger et al. 2006), and even though they can be low
546 abundant, their diversity is striking and underlines their distinct metabolic capabilities (Alves et
547 al. 2018; Huang et al. 2021). Additionally, we compared the detection of *nosZ* genes between the
548 targeted and shotgun metagenomics approaches in the agricultural soil, also based on an existing
549 reference database (Graf et al., 2022). The following datasets were compared: (i) targeted and
550 shotgun metagenomes, and PCR amplicons of the archaeal *amoA* gene in the agricultural soil (Fig.
551 4); (ii) *nosZ* gene sequences identified by targeted or shotgun metagenomics in the agricultural
552 soil (Fig. S3).
553
554 Comparison of results from all three methods in agricultural soil samples showed that targeted
555 metagenomics detected a substantially higher diversity of archaeal *amoA* genes than PCR

556 amplicon sequencing, while, as expected, shotgun metagenomics detected a lower diversity than
557 either of the other two methods (Fig. 4A). Specifically, targeted metagenomics detected 71-83
558 distinct taxonomic bins of *amoA* gene, whereas PCR amplicon sequencing and shotgun
559 metagenomics detected 65-68 taxonomic bins and only three bins, respectively. Rarefaction
560 analysis also indicated that targeted metagenomics retrieved a higher alpha diversity of archaeal
561 *amoA* genes than PCR amplicon sequencing (Fig. 4B,C) and it also reaches a plateau much faster
562 and with a lower number of sequences than amplicon sequencing (Fig. 4B).
563
564 Similarly, targeted metagenomes yielded a higher number of taxonomic bins for *nosZ* genes from
565 the agricultural soil (~6,800 bins) than shotgun metagenomics (~1,300 bins) at a 90% identity
566 cutoff, showing that the first approach detected a greater gene diversity with a much lower
567 sequencing depth (Fig. S3). Gene sequence reads from both methods mapped to similar lineages
568 in a comprehensive reference phylogeny of *nosZ* genes (Graf et al., 2022). However, a greater
569 proportion of reads from the targeted metagenomics approach were assigned to deeper nodes of
570 the phylogeny, particularly within the less studied clade II, suggesting that this method also
571 captured more novel *nosZ* variants not represented in the reference phylogeny.
572
573 Targeted metagenomics with a sequencing depth of 117-160 Mb per sample generated at least
574 2200-4200 times more *TamoA* gene reads than shotgun metagenomics with 7-17 Gb per sample
575 (where only three quality-controlled *amoA* taxonomic bins was detected (Fig 4)). Conversely,
576 targeted metagenomics generated five times less *TamoA* reads (Fig. 4B) than PCR amplicon
577 sequencing, with a sequencing depth of 15-31 Mb per sample. Nevertheless, the targeted
578 metagenomics approach detected a much higher gene sequence diversity for both *TamoA* (Fig 4A,
579 4B) and *nosZ* (Fig. S3) than the two other methods in the agricultural soil samples. For *TamoA*,
580 the targeted approach detected 28 times higher alpha-diversity than shotgun metagenomics, while
581 5 times higher diversity of *nosZ* genes was recovered, importantly covering genes affiliated with
582 the less characterized Clade II. In turn, the targeted approach detected 1.24 times (24% more
583 taxonomic bins) higher diversity of archaeal *amoA* genes than PCR amplicon sequencing in
584 agricultural soils, respectively.
585
586 **Discussion**

587 In this study, we report the development and evaluation of a new probe library for targeted
588 metagenomics of 14 key genes involved in the microbial cycling of inorganic N and CH_4. This
589 included the compilation of databases containing all variants of the target genes from public
590 databases, the development of an extensive set of probes targeting 14 well-established marker
591 genes, and a bioinformatics pipeline to process and annotate the sequence data. This approach has
592 been successfully used earlier to identify genes involved in microbial C metabolism in soil
593 (Manoharan et al., 2015, Manoharan et al., 2017).
594
595 Our custom HMM models could assign reads to the correct genomes based on full protein
596 sequences with higher precision than models based on KEGG Orthologs, especially when used to
597 predict putative functions from short DNA fragments, such as metagenomic reads. This accuracy
598 indicates that the HMMs can reliably classify reads in the mock community and are sensitive
599 enough to detect distantly related genes or novel gene variants. Notably, reads identified as false
600 positives may not actually be incorrect but could represent novel gene variants not captured by
601 KEGG Orthologs.
602
603 In validation experiments with mock communities comprising 18 distinct organisms encoding
604 multiple target genes, we showed that this method successfully reproduced the expected relative
605 abundances of nearly all target genes, with the exception of the *nirK* and *hzoA* genes. Although
606 10.3% of the probes targeted *nirK* genes of nitrifiers, these were detected at a lower relative
607 abundance than that present in the original mock community. However, the relative abundance of
608 *nirK* genes matched the frequency of *nirK* genes only in heterotrophic organisms in the mock
609 community, indicating a bias in the detection of distinct *nirK* gene variants. The sequencing
610 technology used can influence the sequences generated due to known GC biases. In this case, the
611 relative abundance of *nirK* genes may have been biased by the false low coverage of genomic
612 regions with non-optimal GC% content (50-60%) known from MiSeq Illumina sequencing
613 (Browne et al. 2020). Consistent with this observation, there was some variation in probe
614 specificity among mock communities with different genomic GC% content, with high GC%
615 communities having a generally higher target gene detection efficiency. For example, the mean
616 GC% content of nitrifier *nirK* genes is lower than that of heterotrophic *nirK* genes (53% and >60%,
617 respectively) and thus it is plausible that the later are sequenced more efficiently. This effect was

618 also noticeable among *nosZ* genes, as the *nosZ* gene of *D. fermentas*, with GC content of 52.9%
619 (Table S1, Fig. S1), was detected more efficiently than that of *S. denitrificans*, which has a 32.7%
620 GC content. Moreover, variation in detection efficiency may also result from differences in probe
621 hybridization. For instance, probes with higher GC% content are expected to bind more strongly
622 to their targets given the higher binding energy between guanine and cytosine than between
623 adenine and thymine. Although our approach successfully identified *hzoA* genes in the
624 environmental samples, it failed to detect them in mock communities. It is possible that this was
625 due to the PCR-generated genomic fragment used as source material for *hzoA* genes in the mock
626 community, which, unlike other target genes provided in the whole genomic DNA, is more
627 susceptible to degradation or structure-related constraints on probe hybridization.
628
629 Targeted metagenomics also closely reproduced the relative abundances of target genes obtained
630 with shotgun metagenomics in two distinct natural microbial communities from soils. The relative
631 gene abundances were strongly positively correlated between the two methods, indicating that the
632 probe capture step did not introduce a significant quantitative bias. Importantly, this relationship
633 held also true for *nirK* genes, confirming that the lower detection efficiency of nitrifier *nirK* genes
634 was due to a variation in GC content. This observation emphasizes that particular attention should
635 be given to the design of probes for low GC genes, such as by targeting gene regions that are not
636 highly conserved among all gene variants, where higher GC probes are more likely to outcompete
637 lower GC probes, as in the case of *nirK*. Nonetheless, as observed in the mock communities, the
638 relative gene abundances quantified in environmental samples were strongly positively correlated
639 between the two approaches to all GC% categories (Fig. S2). This further supports that the
640 observed variation in detection efficiencies among gene variants with targeted metagenomics has
641 a negligible effect on community profiles.
642
643 The thaumarchaeal *amoA* gene (*TamoA*) and the *nosZ* gene were used as case studies to investigate
644 the differences in the detected diversity of single functional guilds that are known to be highly
645 diverse (Alves et al. 2018, Graf et al. 2022). To determine the community composition of the
646 *TamoA* gene for the different sequencing approaches, the reads are mapped to a reference library,
647 in turn forming the taxonomic bins. Consequently, the same gene from the same organism can be
648 detected multiple times in targeted metagenomics due to multiple probe hybridization. However,

649 when calculation of relative abundance is performed, it balances the detected community because
650 an equal number of probes is used per sequence cluster and therefore the relative abundance of
651 targeted method can be compared to other sequencing tools. At first glance, PCR amplicon
652 sequencing seems to have resulted in 18 more taxonomic bins than targeted metagenomics.
653 However, these sequences were generated by a 35-cycle PCR, known to produce some chimeric
654 sequences. Examples of such errors have been shown even for shorter amplification cycles (Kozich
655 et al., 2013). Problems due to chimeric sequences in public databases from amplicon studies are
656 known and were encountered during the compilation of the thaumarchaeal *amoA* reference
657 database (Alves et al., 2018). Although we used standard pipelines for the detection of chimeric
658 sequences, it is possible that we might have missed some, which may be represented in the 18 bins
659 produced with amplicon sequencing, leading to an inflated number of sequences post-processing.
660 The absence of long amplification steps in targeted metagenomics is expected to preclude the
661 formation of chimeric sequences, which represents a significant advantage over typical PCR-based
662 approaches.
663
664 It should be noted that the efficiency of the targeted metagenomic approach largely depends on the
665 coverage and quality of the database used to generate the probes. We used hmmer profiles to
666 collect all possible genes from the NCBI nucleotide and WGS databases, as well as Fungene and
667 other published databases were used for the target gene library. Only one hmmer profile per gene
668 was used for detection, however, clade specific hmmer profiles could also be used to have a
669 broader outcome for neighbouring clades. We used fairly relaxed conditions when including
670 thresholds for screening the NCBI databases, because we wanted to have closely related organisms
671 and genes in the probe pool. For example, this was the case for the *mmoX* gene family, which also
672 includes butane, propane and toluene monooxygenases. We included these closely related *mmoX*
673 genes in the probes, therefore these closely related *mmoX* genes were found from coniferous trees
674 (Putkinen et al., 2021). However, the database is not constrained to full-length gene sequences
675 from a limited diversity of complete genomes and long metagenomic scaffolds available and the
676 probe/target diversity can be greatly extended through the inclusion of gene fragments generated
677 by PCR or from short metagenomic contigs. Despite its high target precision, this method may
678 nevertheless capture non-target sequences, especially for orthologous gene families who have
679 evolved different functions, as is the case for *napA* genes and formate dehydrogenases. Such cases

680 emphasize the importance of thorough data annotation and filtering procedures. With the target
681 gene database used to generate probes in this study, we managed to detect a higher diversity for
682 the case study of *TamoA* genes than the shotgun sequencing approach, showcasing the advantage
683 of "casting a wider net" with targeted metagenomics. Similar results were obtained in other
684 targeted metagenomics applications, such as for detection of diverse resistome-virulome elements
685 (Noyes et al. 2017) or for improved taxonomic microbial community characterization via 16S
686 rRNA enrichment (Beaudry et al. 2021).
687
688 Despite the technological advances and decline in cost of high-throughput sequencing, shotgun
689 metagenomics remain impractical and prohibitively expensive to capture the diversity of specific,
690 low abundant functional groups in complex environments, such as soils and sediments, especially
691 in longitudinal studies. The current cost of generating the probes for targeted metagenomics is
692 about 20-50 € per sample depending on the probe manufacturer. If the goal is to have a focused,
693 comprehensive view of the diversity of functional guilds involved in inorganic nitrogen or methane
694 cycling in a certain ecosystem, then targeted metagenomics can circumvent the high cost and
695 overabundance of data generated by shotgun metagenomics, as well as provide more quantitative
696 data and more information on the diversity of the genes of interest. In turn, PCR-based assays are
697 limited by the biases associated with any set of primers targeting a large diversity of sequences,
698 assay efficiencies which preclude the detection of highly divergent new sequence diversity as well
699 as known issues with the generation of chimeric sequences during amplification. The targeted
700 metagenomics approach circumvents these limitations by using multiple short probes targeting
701 different regions of each gene, which largely increases the likelihood of capturing sequence
702 variants that elude PCR amplification. Thus, this approach has not only the potential to capture
703 rare and novel gene diversity in complex environments, but also to identify cryptic microorganisms
704 in low-biomass samples or involved in suggested CH_4 metabolisms, such as in the tree
705 phyllosphere (Putkinen et al., 2021) and nitrogen cycling in coral holobiont (Glaze et al., 2021).
706 Moreover, targeted metagenomics can also overcome issues associated with running and
707 comparing multiple independent PCR assays when investigating several distinct targets. In that
708 sense, this approach effectively represents a PCR-independent, multiplex approach to characterize
709 simultaneously and in-depth the distributions of a broad range of functional genes, providing a
710 holistic view of the status of the nitrogen and methane cycles in the studied ecosystems. This is

711 especially advantageous when combined with functional studies, such as the determination of N-
712 transformation rates and *in situ* fluxes, as showcased by a study of N_2O emissions in thawing
713 Yedoma permafrost sites over time (Maruschak et al. 2021). In this study, the application of
714 targeted metagenomics with the N-cycling probe dataset presented here revealed that changes in
715 the N-cycling microbial community composition were responsible for an increase in N_2O
716 emissions in revegetated Yedoma soils, which had undergone thawing a decade prior.
717
718 Conclusively, the targeted metagenomics approach developed here provides an efficient and cost-
719 effective strategy for studying microbial functional guilds that typically represent small fractions
720 of natural microbiomes, and whose diversity is generally underestimated and highly
721 underrepresented in metagenomic datasets. This approach also circumvents the limitations and
722 biases associated with PCR-based methods and has higher potential to capture rare or novel
723 functional gene diversity.
724
725
726
727 **Acknowledgements**
728 H.S. was financially supported by the Atmosphere and Climate Competence Center (ACCC)
729 Academy of Finland project number 337550, and Nitrobiome project 342362, in addition H.S. was
730 supported by Saastamoinen foundation, FEMS Society and Niemi foundation. L.M., A.B., and
731 C.S. were funded by ERC Advanced Grant TACKLE (695192), and R.J.E.A. was funded by
732 project P25369 of the Austrian Science Fund (FWF). A.S.H and F.L.S were funded by ERC
733 Starting Grant EvolPhisiol (grant agreement 803768). S.H and C.M.J were supported by the
734 Swedish University of Agricultural Sciences (senior career grant 2019-2024). We thank Lea
735 Wittorf for providing DNA extracts from isolates for the mock libraries.
736

737 **Authors contribution statement**

738 H.S., C.S., R.A. designed study, H.S. collected the targeted gene library, R.A.,S.H.,C.J. provided
739 reference libraries for *amoA* and *nosZ* genes, L.M. designed the probes, L.M., A.B., H.S. extracted
740 the environmental DNA and did the shotgun metagenomics, H.S. and S.H. extracted and provided

741 the mock sample cultured organisms, A.H., F.S. did the precision and recall analysis between the
742 KEGG and HMM approaches, A.B., H.S. did the *amoA* diversity comparison, S.H.,C.J. did the
743 *nosZ* diversity comparison. H.S. wrote the first version of manuscript and all co-authors further
744 developed the text.

745 **References:**

746

747 Aanderud, Z.T., Jones, S.E., Fiererr, N., Lennon, J.T. 2015. Resuscitation of the rare biosphere
748 contributes to pulses of ecosystem activity. *Front Microbiol* 6: DOI=10.3389/fmicb.2015.00024

749

750 Alteio, L.V., Séneca, J., Canarini, A., Angel, R., Jansa J., Guseva, K., Kaiser, C., Richter, A.,
751 Schmidt, H. 2021. A critical perspective on interpreting amplicon sequencing data in soil
752 ecological research. *Soil Biol Biochem* 160:108357,
753 https://doi.org/10.1016/j.soilbio.2021.108357.

754

755 Altschul, S. F., Gish, W., Miller, W., Myers, E. W., Lipman, D. J. 1990. Basic local alignment
756 search tool. *J. Mol. Biol.* 215: 403-410.

757

758 Alves, R.J.E., Minh, B.Q., Urich, T., von Haeseler, A., Schleper, C. 2018. Unifying the global
759 phylogeny and environmental distribution of ammonia-oxidizing archaea based on amoA genes.
760 *Nat. Comm.* 9: 1517. https://doi.org/10.1038/s41467-018-03861-1.

761

762 Archer, D. 2010. The Global Carbon Cycle. Princeton: Princeton University Press. ISBN
763 9781400837076.

764

765 Aramaki, T., Blanc-Mathieu, R., Endo, H., Ohkubo, K., Kanehisa, M., Goto, S., Ogata, H. 2020.
766 KofamKOALA: KEGG Ortholog assignment based on profile HMM and adaptive score threshold.
767 *Bioinform.* 36:2251-2252. Doi: 10.1093/bioinformatics/btz859.

768

769 Barnard, R., Leadley, P. W., and Hungate, B. A. (2005), Global change, nitrification, and
770 denitrification: A review. *Glob. Biogeochem. Cycles* 19, GB1007, doi:10.1029/2004GB002282.

771

Beaudry, M.S. et al. (2021) Improved Microbial Community Characterization of 16S rRNA via Metagenome Hybridization Capture Enrichment. *Front. Microbiol.* 12. Available at: https://doi.org/10.3389/fmicb.2021.644662.

Barbera, P., Kozlov, A.M., Czech, L., Morel, B., Darriba, D., Flouri, T., Stamatakis, A. 2019. EPA-ng: Massively Parallel Evolutionary Placement of Genetic Sequences. *Syst. Biol.* 68: 365-369.

Bewicke-Copley, F., Arjun Kumar, E., Palladino, G., Korfi, K., Wang, J. 2019. Applications and analysis of targeted genomic sequencing in cancer studies. *Comput. Struct. Biotechnol. J.* 17:1348-1359. Doi: 10.1016/j.csbj.2019.10.004.

Buchfink, B., Xie, C., Huson, D. H. 2015. Fast and sensitive protein alignment using DIAMOND. *Nat. methods.* 12: 59.

Bodelier, P.L.E., Laanbroek, H.J. 2004. Nitrogen as a regulatory factor of methane oxidation in soils and sediments. *FEMS Microbiol. Ecol.* 47: 265–277, https://doi.org/10.1016/S0168-6496(03)00304-0

Bonilla-Rosso, G., Wittorf, L., Jones, C. *et al.* 2016. Design and evaluation of primers targeting genes encoding NO-forming nitrite reductases: implications for ecological inference of denitrifying communities. *Sci. Rep.* 6: 39208 https://doi.org/10.1038/srep39208

Borrel, G., Adam, P.S., McKay, L.J. *et al.* Wide diversity of methane and short-chain alkane metabolisms in uncultured archaea. *Nat. Microbiol.* **4**, 603–613 (2019). https://doi.org/10.1038/s41564-019-0363-3

Browne, P.D. Nielsen. T.K., Kot, W., Aggerholm, A., Thomas, M., Gilbert, P., Puetz, L., Rasmussen, M., Zervas, A., Hansen L.H. 2020. GC bias affects genomic and metagenomic reconstructions, underrepresenting GC-poor organisms. *GigaScience* 9: giaa008, https://doi.org/10.1093/gigascience/giaa008

Bräuer, S.L,, Basiliko, N., Siljanen, H.M.P., Zinder, S.H. 2021. Methanogenic archaea in peatlands. *FEMS Microbiol. Lett*. 367: fnaa172, https://doi.org/10.1093/femsle/fnaa172

Callahan, B.J., McMurde, P.J., Rosen, M.J., Han, A.W., Johnson, A.J., Holmes, S.P., 2016. DADA2: high-resolution sample inference from Illumina amplicon data. *Nat. Methods* 13: 581–583. https://doi.org/10.1038/nmeth.3869.

Caporaso, J.G., Kuczynski, J., Stombaugh, J., Bittinger, K., Bushman, F.D., Costello, E.K., Fierer, N., Gonzalez Peña, A., Goodrich, J.K., Gordon, J.I., Huttley, G.A., Kelley, S.T., Knights, D., Koenig, J.E., Ley, R.E., Lozupone, C.A., McDonald, D., Muegge, B.D., Pirrung, M., Reeder, J., Sevinsky, J.R., Turnbaugh, P.J., Walters, W.A., Widmann, J., Yatsunenko, T., Zeneveld, J., Knight, R., 2010. QIIME allows analysis of Highthroughput community sequencing data. *Nat. Methods* 7: 335–336.

Cerqueira, N.M.F.S.A., Gonzalez, P.J., Fernandes, P.A., Moura, J.J.G., Ramos, M.A. 2015. Periplasmic Nitrate Reductase and Formate Dehydrogenase : Similar Molecular Architectures with Very Different Enzymatic Activities. *Acc. Chem. Res.* 48: 2875-2884 DOI: 10.1021/acs.accounts.5b00333

Clark, D.R., McKew, B.A., Binley, A. et al. 2022. Hydrological properties predict the composition of microbial communities cycling methane and nitrogen in rivers. *ISME Commun.* 2: 5 https://doi.org/10.1038/s43705-022-00087-7

Cleary, B. et al. 2015. Detection of low-abundance bacterial strains in metagenomic datasets by eigengenome partitioning. *Nat. Biotech.* 33: 1053–1060. https://doi.org/10.1038/nbt.3329.

Conrad, R. 2009. The global methane cycle: recent advances in understanding the microbial processes involved. *Environ. Microbiol. Rep.* 1: 285-292. https://doi.org/10.1111/j.1758-2229.2009.00038.x

Friedlingstein, P., O'Sullivan, M., Jones, M. W., Andrew, R. M., Hauck, J., Olsen, A., Peters, G. P., Peters, W., Pongratz, J., Sitch, S., Le Quéré, C., Canadell, J. G., Ciais, P., Jackson, R. B., Alin, S., Aragão, L. E. O. C., Arneth, A., Arora, V., Bates, N. R., Becker, M., Benoit-Cattin, A., Bittig, H. C., Bopp, L., Bultan, S., Chandra, N., Chevallier, F., Chini, L. P., Evans, W., Florentie, L., Forster, P. M., Gasser, T., Gehlen, M., Gilfillan, D., Gkritzalis, T., Gregor, L., Gruber, N., Harris, I., Hartung, K., Haverd, V., Houghton, R. A., Ilyina, T., Jain, A. K., Joetzjer, E., Kadono, K., Kato, E., Kitidis, V., Korsbakken, J. I., Landschützer, P., Lefèvre, N., Lenton, A., Lienert, S., Liu, Z., Lombardozzi, D., Marland, G., Metzl, N., Munro, D. R., Nabel, J. E. M. S., Nakaoka, S.-I., Niwa, Y., O'Brien, K., Ono, T., Palmer, P. I., Pierrot, D., Poulter, B., Resplandy, L., Robertson, E., Rödenbeck, C., Schwinger, J., Séférian, R., Skjelvan, I., Smith, A. J. P., Sutton, A. J., Tanhua, T., Tans, P. P., Tian, H., Tilbrook, B., van der Werf, G., Vuichard, N., Walker, A. P., Wanninkhof, R., Watson, A. J., Willis, D., wiltshire, A. J., Yuan, W., yue, X., and Zaehle, S. 2020. Global Carbon Budget. *Earth Syst. Sci. Data* 12: 3269–3340, https://doi.org/10.5194/essd-12-3269-2020, 2020.

Falkowski, P.; Scholes, R. J.; Boyle, E.; Canadell, J.; Canfield, D.; Elser, J.; Gruber, N.; Hibbard, K.; Högberg, P.; Linder, S.; MacKenzie, F. T.; Moore b, 3.; Pedersen, T.; Rosenthal, Y.; Seitzinger, S.; Smetacek, V.; Steffen, W. 2000. The Global Carbon Cycle: A Test of Our Knowledge of Earth as a System. *Science.* 290: 291–296. Doi:10.1126/science.290.5490.291

Futema, M., Plagnol, V., Whittall, R.A., et al. 2012. Use of targeted exome sequencing as a diagnostic tool for Familial Hypercholesterolaemia. *J. Med. Genet.* 49:644-649.

Galloway, J. N., Dentener, F. J., Capone, D. G., Boyer, E. W., Howarth, R. W., Seitzinger, S. P., G. P. Asner, C. C. Cleveland, P. A. Green, Holland, E. A., Karl, D. M., Michaels, A. F., Porter, J. H., Townsend, A. R., & Vörösmarty, C. J. (2004). Nitrogen Cycles: Past, Present, and Future. *Biogeochemistry* 70: 153–226. http://www.jstor.org/stable/4151466

Gasc, C., Peyretaillade, E. and Peyret, P. (2016) Sequence capture by hybridization to explore modern and ancient genomic diversity in model and nonmodel organisms. *Nucleic. Acids Res.* 44: 4504–4518. https://doi.org/10.1093/nar/gkw309.

Graf, D.R., Jones, C.M., Hallin, S. 2014. Intergenomic comparisons highlight modularity of the denitrification pathway and underpin the importance of community structure for N_2O emissions. *PloS one* 9: e114118.

869 Graf, D.R.H., Jones, C.M., Zhao, M., Hallin, S. 2022. Assembly of root-associated N2O-reducing
870 communities of annual crops is governed by selection for nosZ clade I over clade II. *FEMS*
871 *Microbiol. Ecol.* 98:1-11
872
873 Gruber, N., Galloway, J. An Earth-system perspective of the global nitrogen cycle. 2008. *Nature*
874 451, 293–296. https://doi.org/10.1038/nature06592
875
876 Glaze, T.D., Erler, D.V., Siljanen, H.M.P. 2021. Microbially facilitated nitrogen cycling in tropical
877 corals. *ISME J.* 16: 68–77 doi: 10.1038/s41396-021-01038-1.
878
879 Eddy, S.R.. 1998. Profile hidden Markov models. *Bioinformatics* 14: 755–763,
880 https://doi.org/10.1093/bioinformatics/14.9.755
881
882 Eddy S.R. 2011. Accelerated profile HMM searches. *PLOS Comp. Biol.*, 7:e1002195, 2011
883
884 Edgar, R.C., 2010. Search and clustering orders of magnitude faster than BLAST. *BMC*
885 *Bioinformatics* 26: 2460–2461
886
887 Edgar, R.C., Haas, B.J., Clemente, J.C., Quince, C., Knight, R., 2011. UCHIME improves
888 sensitivity and speed of chimera detection. *BMC Bioinformatics* 27: 2194–2200.
889
890 Fish, J. A., Chai, B., Wang, Q., Sun, Y., Brown, C. T., Tiedje, J. M., Cole, J. R. 2013.
891 FunGene: the Functional Gene Pipeline and Repository. *Front. Microbiol.* 4: 291.
892
893 Hallin S, Lindgren PE. 1999. PCR detection of genes encoding nitrite reductase in denitrifying
894 bacteria. *Appl Environ Microbiol.* 65:1652-7. doi: 10.1128/AEM.65.4.1652-1657.1999.
895
896 Hoang, D.T., Chernomor, O., Von Haeseler, A. et al. 2018. UFBoot2: improving the ultrafast
897 bootstrap approximation. *Mol Biol Evol* 35:518
898

899 Huang, L., Chakrabarti, S., Cooper, J., Perez,A., John, S.M., Daroub, S.H., Martens-Habbena,
900 W. 2021. Ammonia-oxidizing archaea are integral to nitrogen cycling in a highly fertile
901 agricultural soil. *ISME Comm.* 1:19 ; https://doi.org/10.1038/s43705-021-00020-4
902
903 Håvelsrud, O.E., Haverkamp, T.H., Kristensen, T. *et al.* A metagenomic study of methanotrophic
904 microorganisms in Coal Oil Point seep sediments. *BMC Microbiol* **11**, 221 (2011).
905 https://doi.org/10.1186/1471-2180-11-221
906
907 Hyatt, D., Chen, G.L., LoCascio, R.F. *et al.* 2010. Prodigal: prokaryotic gene recognition and
908 translation initiation site identification. *BMC Bioinformatics* 11: 119 https://doi.org/10.1186/1471-
909 2105-11-119
910
911 Ichida, H., Morita, R., Shirakawa, Y., Hayashi, Y., Abe, T. 2019. Targeted exome sequencing of
912 unselected heavy-ion beam-irradiated populations reveals less-biased mutation characteristics in
913 the rice genome. *Plant J.* 98:301-314. Doi: 10.1111/tpj.14213.
914
915 Jones, C.M., Graft, D.R.H., Bru, D., Philippot, L., Hallin, S. 2013. The unaccounted yet abundant
916 nitrous oxide-reducing microbial community: a potential nitrous oxide sink. *ISME J* 7: 417-426.
917
918 Kalyaanamoorthy, S., Minh, B.Q., Wong, T.K. et al. 2017. ModelFinder: fast model selection for
919 accurate phylogenetic estimates. *Nat. Methods* 14:587–9.
920
921 Kamil, G., Yoon, J.Y., Yoo, S. et al. 2021. Clinical relevance of targeted exome sequencing in
922 patients with rare syndromic short stature. *Orphanet J Rare Dis* 16: 297
923 https://doi.org/10.1186/s13023-021-01937-8
924
925 Katoh, K., Rozewicki, J., Yamada, K.D. 2019. MAFFT online service: multiple sequence
926 alignment, interactive sequence choice and visualization. *Brief Bioinform* 20: 1160–66.
927

928 Knief, C. 2015. Diversity and Habitat Preferences of Cultivated and Uncultivated Aerobic
929 Methanotrophic Bacteria Evaluated Based on *pmoA* as Molecular Marker. *Front Microbiol* 6:1346.
930 Doi: 10.3389/fmicb.2015.01346
931
932 Kushwaha, S.K., Manoharan, L., Meerupati, T., Hedlund, K., & Ahrén, D. 2015. MetCap: a
933 bioinformatics probe design pipeline for large-scale targeted metagenomics. *BMC bioinformatics*
934 16: 65.
935
936 Kuypers, M., Marchant, H. & Kartal, B. 2018. The microbial nitrogen-cycling network. *Nat Rev*
937 *Microbiol* 16: 263–276. https://doi.org/10.1038/nrmicro.2018.9
938
939 Kolb S, Knief C, Stubner S, Conrad R. 2003. Quantitative detection of methanotrophs in soil by
940 novel pmoA-targeted real-time PCR assays. *Appl Environ Microbiol.* 69:2423-9. Doi:
941 10.1128/AEM.69.5.2423-2429.2003.
942
943 Lan, X., K.W. Thoning, and E.J. Dlugokencky: Trends in globally-averaged CH4, N2O, and SF6
944 determined from NOAA Global Monitoring Laboratory measurements. Version 2023-09,
945 https://doi.org/10.15138/P8XG-AA10
946
947 Letunic, I, Bork, P. 2019. Interactive Tree Of Life (iTOL) v4: recent updates and new
948 developments. *Nucleic Acids Res* 47:W256–9
949
950 Li, J., Liu, T., McIlroy, S.J. et al. 2023. Phylogenetic and metabolic diversity of microbial
951 communities performing anaerobic ammonium and methane oxidations under different nitrogen
952 loadings. *ISME Commun.* 3, 39. https://doi.org/10.1038/s43705-023-00246-4
953
954 Liu, F., Zhang, J. & Mei, Y. 2016. The origin of the cooperativity in the streptavidin-biotin system:
955 A computational investigation through molecular dynamics simulations. *Sci. Rep.* 6, 27190.
956 https://doi.org/10.1038/srep27190
957
958 Ludwig, W., Strunk, O., Westram, R., et al. 2004. ARB: a software environment for sequence data. *Nucleic*
959 *Acids Res.* 32: 1363-1371.

Manoharan, L., Kushwaha, S. K., Hedlund, K., Ahrén, D. (2015). Captured metagenomics: large-scale targeting of genes based on 'sequence capture' reveals functional diversity in soils. *DNA Res.* 22: 451-460.

Manoharan, L., Kushwaha, S.K., Ahrén, D., Hedlund, K. 2017. Agricultural land use determines functional genetic diversity of soil microbial communities. *Soil Biol Biochem* 115: 423-432

Morris A., Meyer K., Bohannan B. 2020. Linking microbial communities to ecosystem functions: what we can learn from genotype–phenotype mapping in organisms. *Phil. Trans. R. Soc.* B3752019024420190244. https://doi.org/10.1038/s41467-021-21400-3

Murrell, J.C., Jetten, M.S.M. 2009. The microbial methane cycle. *Environ Microb Rep* 1: 279-284. https://doi.org/10.1111/j.1758-2229.2009.00089.x

Myhre, G.G.D., Shindell, F.M., Bréon, W., Collins, J., Fuglestvedt, J., Huang, J., Koch, D.,Lamarque, J.F., Lee, D., Mendoza, B., Nakajima, T., Robock, A., Stephens, G., Takemura, T., Zhang, H., 2013. Anthropogenic and natural radiative forcing. In:Stocker, T.F., Qin, D., Plattner, G.K., Tignor, M., Allen, S.K., Boschung, J., Nauels, A.,Xia, Y., Bex, V., Midgley, P.M. (Eds.), Climate Change 2013 the Physical ScienceBasis. Cambridge University Press, Cambridge, United Kingdom and New York, NY,USA Working Group I Contribution to the Fifth Assessment Report of the Intergovernmental Panel on Climate Change.

Nelson, M.B., Martiny , A.C., Martiny, J.B.H. 2016. Global biogeography of microbial nitrogen-cycling traits in soil. *PNAS* 113 (29) 8033-8040. https://doi.org/10.1073/pnas.1601070113

Nguyen, L.T., Schmidt, H.A., von Haeseler, A. et al. 2015. IQ-TREE: a fast and effective stochastic algorithm for estimating maximum-likelihood phylogenies. *Mol Biol Evol* 32:268–74.

Nnadozie, C.F., Lin, J. and Govinden, R. (2015) 'Selective isolation of bacteria for metagenomic analysis: Impact of membrane characteristics on bacterial filterability'. *Biotechnol Prog.* 31: 853–866. https://doi.org/10.1002/btpr.2109.

992
993 Noyes, N.R. et al. (2017) Enrichment allows identification of diverse, rare elements in
994 metagenomic resistome-virulome sequencing. *Microbiome* 5. 142.
995 https://doi.org/10.1186/s40168-017-0361-8.
996
997 R Core Team 2018. R: A language and environment for statistical computing. R Foundation for
998 Statistical Computing, Vienna, Austria. URL https://www.R-project.org/.
999
1000 Rice P, Longden I, Bleasby A. 2000. EMBOSS: the European Molecular Biology Open Software
1001 Suite. Trends Genet. 16: 276-7. doi: 10.1016/s0168-9525(00)02024-2. PMID: 10827456.
1002
1003 Romdhane, S., Spor, A., Aubert, J. *et al.* 2021. Unraveling negative biotic interactions determining
1004 soil microbial community assembly and functioning. *ISME J.* https://doi.org/10.1038/s41396-021-
1005 01076-9
1006
1007 Palmer, K., Biasi, C., Horn, M.A. 2012. Contrasting denitrifier communities relate to contrasting
1008 N_2O emissions patterns from acidic peat soils in arctic tundra. *ISME J.* 6:1058-1077.
1009
1010 Parks, D.H., Imelfort, M., Skennerton, C.T., Hugenholtz, P., Tyson, G.W., 2015. CheckM: assessing the
1011 quality of microbial genomes recovered from isolates, single cells, and metagenomes. *Genome Res.* 25:
1012 1043-1055.
1013
1014 Pan Y, Bodrossy L, Frenzel P, Hestnes AG, Krause S, Lüke C, Meima-Franke M, Siljanen H,
1015 Svenning MM, Bodelier PL. Impacts of inter- and intralaboratory variations on the reproducibility
1016 of microbial community analyses. *Appl Environ Microbiol.* 2010 Nov;76(22):7451-8. doi:
1017 10.1128/AEM.01595-10
1018
1019 Price, M.N., Dehal, P.S., Arkin, A.P., 2010. FastTree 2--approximately maximum-likelihood trees for
1020 large alignments. *PLoS ONE* 5: e9490.
1021

1022 Prosser, JI, Hink, L, Gubry-Rangin, C, Nicol, GW. Nitrous oxide production by ammonia
1023 oxidizers: Physiological diversity, niche differentiation and potential mitigation strategies. Glob
1024 Change Biol. 2020; 26: 103– 118. https://doi.org/10.1111/gcb.14877
1025
1026 Putkinen, A., Siljanen, H.M.P., Laihonen, A., Paasisalo, I., Porkka, K., Tiirola, M., Haikarainen,
1027 I., Tenhovirta, S. and Pihlatie, M. 2021. New insight to the role of microbes in the methane
1028 exchange in trees: evidence from metagenomic sequencing. *New Phytol* 231: 524-536.
1029 https://doi.org/10.1111/nph.17365
1030
1031 Saghaï, A., Pold, G., Jones, C.M., Hallin, S. 2023. Phyloecology of nitrate ammonifiers and their
1032 importance relative to denitrifiers in global terrestrial biomes. *Nature Communications*, 14:8249
1033
1034 Skoglund, P., et al. 2014. Separating endogenous ancient DNA from modern day contamination
1035 in a Siberian Neandertal. *Proc Natl Acad Sci USA* 111: 2229–2234 .

1036 Siljanen, H.M.P., Alves, R.J.E., Ronkainen, J.G., Lamprecht, R.E., Bhattarai, H.R., Bagnoud, A.,
1037 Marushchak, M.E., Martikainen, P.J. Schleper, C., Biasi, C. 2019. Archaeal nitrification is a key driver of
1038 high nitrous oxide emissions from arctic peatlands. *Soil Biol Biochem* 137: 107539
1039
1040 Siljanen, H.M.P., Saari, A., Krause, S., Lensu, A., Abell, G.C.J., Bodrossy, L., Bodelier, P.L.E.,
1041 Martikainen, P.J. 2011. Hydrology is reflected in the functioning and community composition of
1042 methanotrophs in the littoral wetland of a boreal lake. *FEMS Microbiol Ecol*. 75:430–445,
1043 https://doi.org/10.1111/j.1574-6941.2010.01015.x
1044
1045 Sinha, R. et al. 2017. Assessment of variation in microbial community amplicon sequencing by
1046 the Microbiome Quality Control (MBQC) project consortium. *Nature Biot* 35: 1077–1086.
1047 https://doi.org/10.1038/nbt.3981.
1048
1049 Stamatakis, A. 2014 RAxML Version 8: a tool for phylogenetic analysis and post-analysis of large
1050 phylogenies. *Bioinformatics* 30:1312–13.
1051

1052 Stein, L.Y., Klotz, M.G. 2016. The nitrogen cycle. *Curr Biol.* 26: R94-R98,
1053 https://doi.org/10.1016/j.cub.2015.12.021.
1054
1055 Sui, H.Y. et al. (2020) Impact of DNA Extraction Method on Variation in Human and Built
1056 Environment Microbial Community and Functional Profiles Assessed by Shotgun Metagenomics
1057 Sequencing. *Front Microb.* 11: . Available at: https://doi.org/10.3389/fmicb.2020.00953
1058
1059 Trifinopoulos, J., Nguyen, L.T., von Haeseler, A., Minh, B.Q. 2016. W-IQ-TREE: a fast online
1060 phylogenetic tool for maximum likelihood analysis. *Nucleic Acids Res.* 44(W1):W232-5. doi:
1061 10.1093/nar/gkw256.
1062
1063 Thomson R.A.J., Giannopoulos, G., Pretty, J., Baggs, E.M., David J. 2012. Biological sources
1064 and sinks of nitrous oxide and strategies to mitigate emissions. *Phil. Trans. R. Soc. B* 2012 367,
1065 doi: 10.1098/rstb.2011.0415, published 26 March 2012
1066
1067 Throbäck, I.N., Enwall, K., Jarvis, Å. and Hallin, S. 2004. Reassessing PCR primers targeting nirS,
1068 nirK and nosZ genes for community surveys of denitrifying bacteria with DGGE. *FEMS Microbiol*
1069 *Ecol* 49: 401-417. https://doi.org/10.1016/j.femsec.2004.04.011
1070
1071 Orellana, L.H., Hatt, J.K., Iyer, R. *et al.* Comparing DNA, RNA and protein levels for measuring
1072 microbial dynamics in soil microcosms amended with nitrogen fertilizer. *Sci Rep.* **9**, 17630 (2019).
1073 https://doi.org/10.1038/s41598-019-53679-0
1074
1075 Ouyang Y., Norton J.M. 2020. Nitrite Oxidizer Activity and Community Are More Responsive
1076 Than Their Abundance to Ammonium-Based Fertilizer in an Agricultural Soil. *Front Microbiol.*
1077 11: DOI=10.3389/fmicb.2020.01736
1078
1079 Wheeler, T.J., Eddy, S.R. 2013. nhmmer: DNA homology search with profile HMMs.
1080 *Bioinformatics* 29: 2487-2489.
1081

1082 Yu, G.C., Smith, D.K., Zhu, H.C., Guan, Y., Lam, T.T.Y. 2017. GGTREE: an R package for visualization
1083 and annotation of phylogenetic trees with their covariates and other associated data. *Methods in Ecol Evol.*
1084 8: 28-36.
1085
1086 Zaehle S. 2013.Terrestrial nitrogen–carbon cycle interactions at the global scale. Phil. Trans. R.
1087 Soc. B3682013012520130125 http://doi.org/10.1098/rstb.2013.0125
1088
1089 Zhao, J., Huang, L., Chakrabarti, S. et al. 2023. Nitrogen and phosphorous acquisition strategies
1090 drive coexistence patterns among archaeal lineages in soil. *ISME J.* 17, 1839–1850
1091 https://doi.org/10.1038/s41396-023-01493-y
1092
1093

1094 **Figures:**

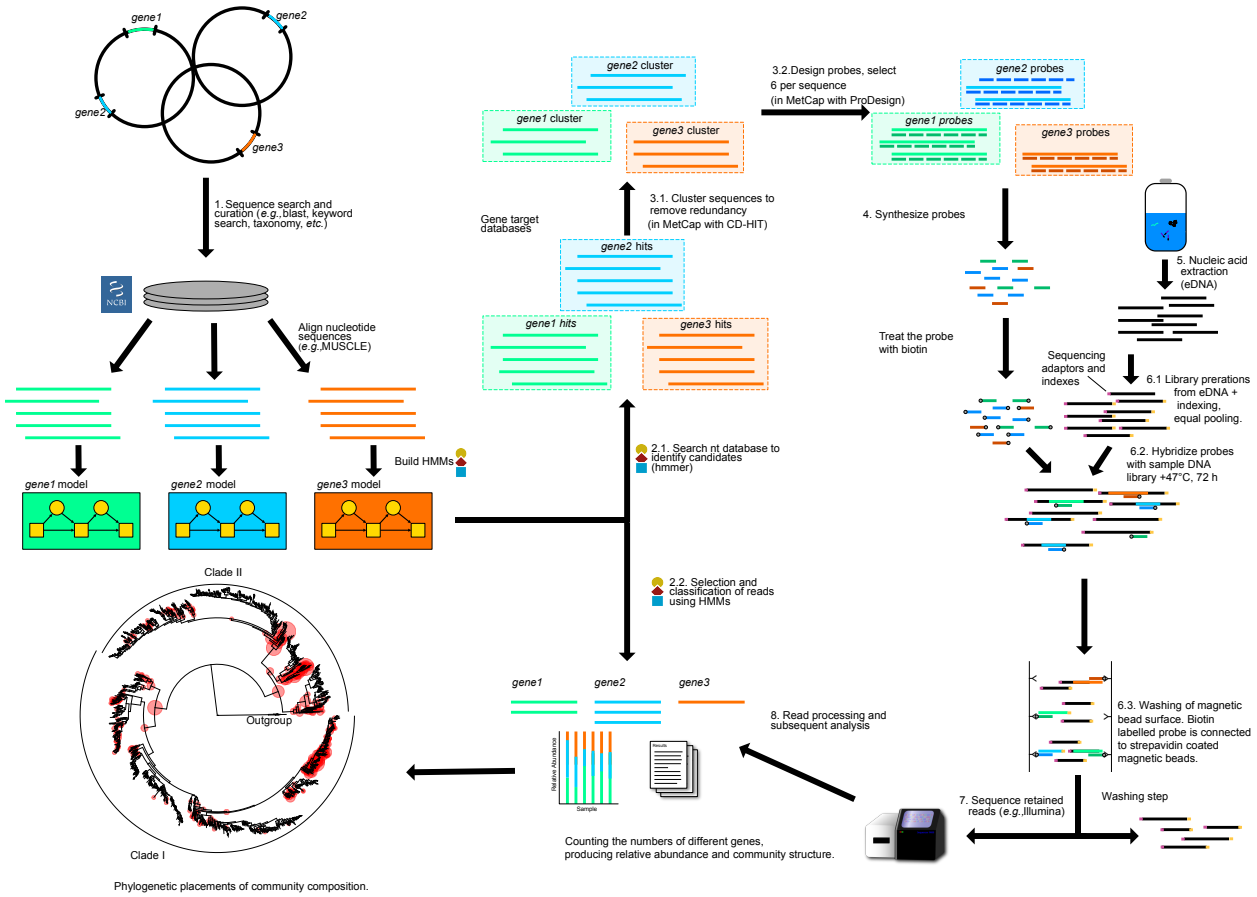

1095

1096 Fig. 1 Illustration of the pipeline for the generation of HMM models for each gene, and how these
1097 models are used to study community composition with targeted metagenomics: 1. Steps followed
1098 for the generation of sequence databases for the genes of interest and subsequent building of the
1099 respective HMM models for each gene; 2.1. The produced HMM models were used to recruit more
1100 gene variants from the NCBI nt database and generate a target gene database for probe design; 2.2.
1101 The same HMM models were also used to classify the reads captured downstream; 3.1. Clustering
1102 of the target gene database with CD-HIT (in MetCap pipeline); 3.2. Design and selection of six
1103 50-mer probes for each sequence cluster (in MetCap pipeline); 4. Synthesis and biotinylation of
1104 the designed probes by Roche; 5. DNA extraction of the sample of interest; 6.1. Sequencing
1105 libraries preparation and addition of sequencing adaptors and indexes; 6.2. Hybridization of the
1106 probes to indexed DNA libraries for 72 hours at +47°C; 6.3. Purification of the DNA hybridized
1107 to the probes with streptavidin coated magnetic beads; 7. Sequencing of the hybridized libraries

with Illumina MiSeq; 8. Read processing with HMM profiles and taxonomy assignment for the genes of interest.

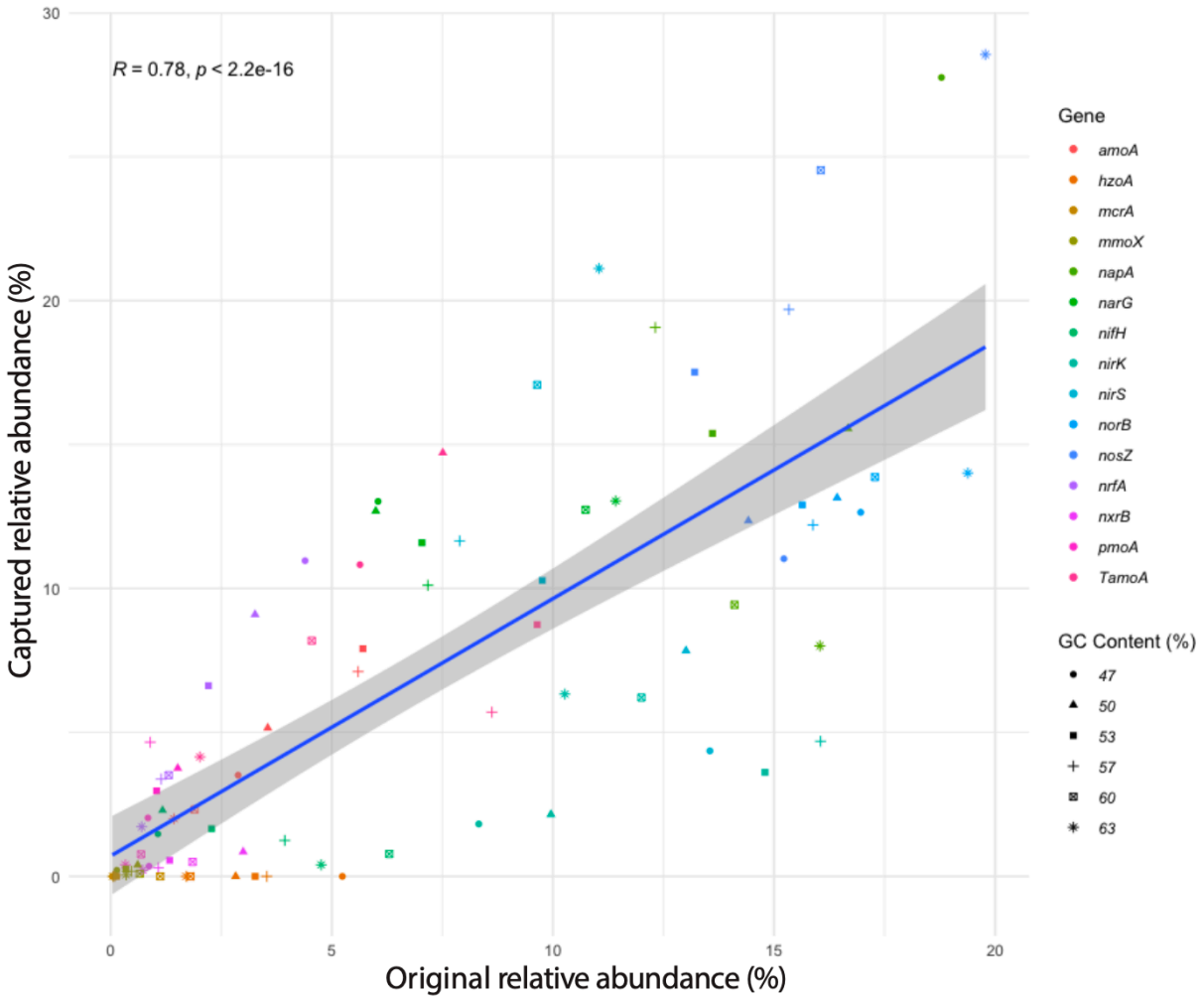

Fig. 2. Comparison between the original composition (DNA of strains applied into the mock sample) of the mock community and the relative abundance for each functional gene detected using probe captured metagenomics for all GC% combinations combined. The relative abundance in the mock community was calculated based on the amount of each functional gene and organism as well as genome size. Color of the symbols depict gene and shape depicts the category of GC content (%).

1121

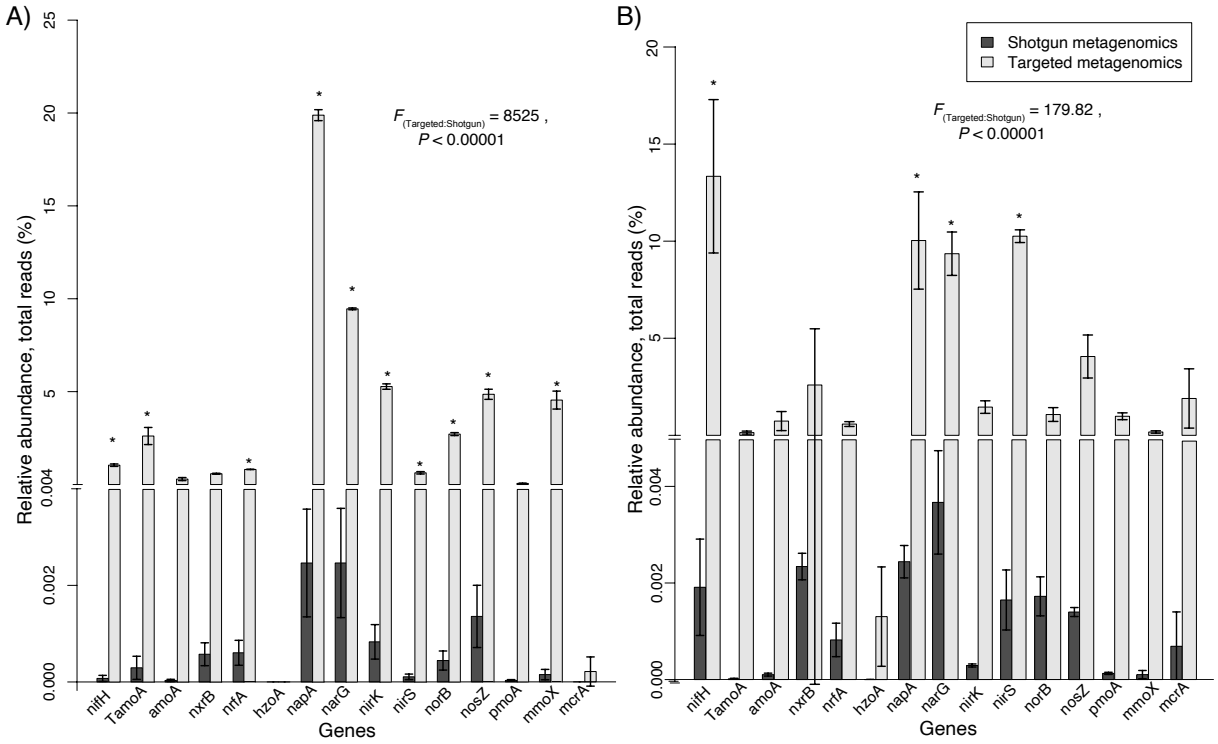

1122

1123 Fig. 3. The relative abundance of functional genes (calculated against total sequencing reads)
1124 involved in inorganic nitrogen and methane cycling obtained by targeted metagenomics and
1125 shotgun metagenomics from A) agricultural soil; and B) wetland soil. Relative abundance was
1126 retrieved with HMMER searches of each functional gene. Statistically significant differences
1127 between shotgun and targeted relative abundances according to pairwise comparisons with
1128 ANOVA are shown with asterisk (P < 0.05, n = 3). The comparison of shotgun vs. targeted
1129 metagenomic measured with ANOVA is shown as F values and significance in the inset for both
1130 samples.

1131

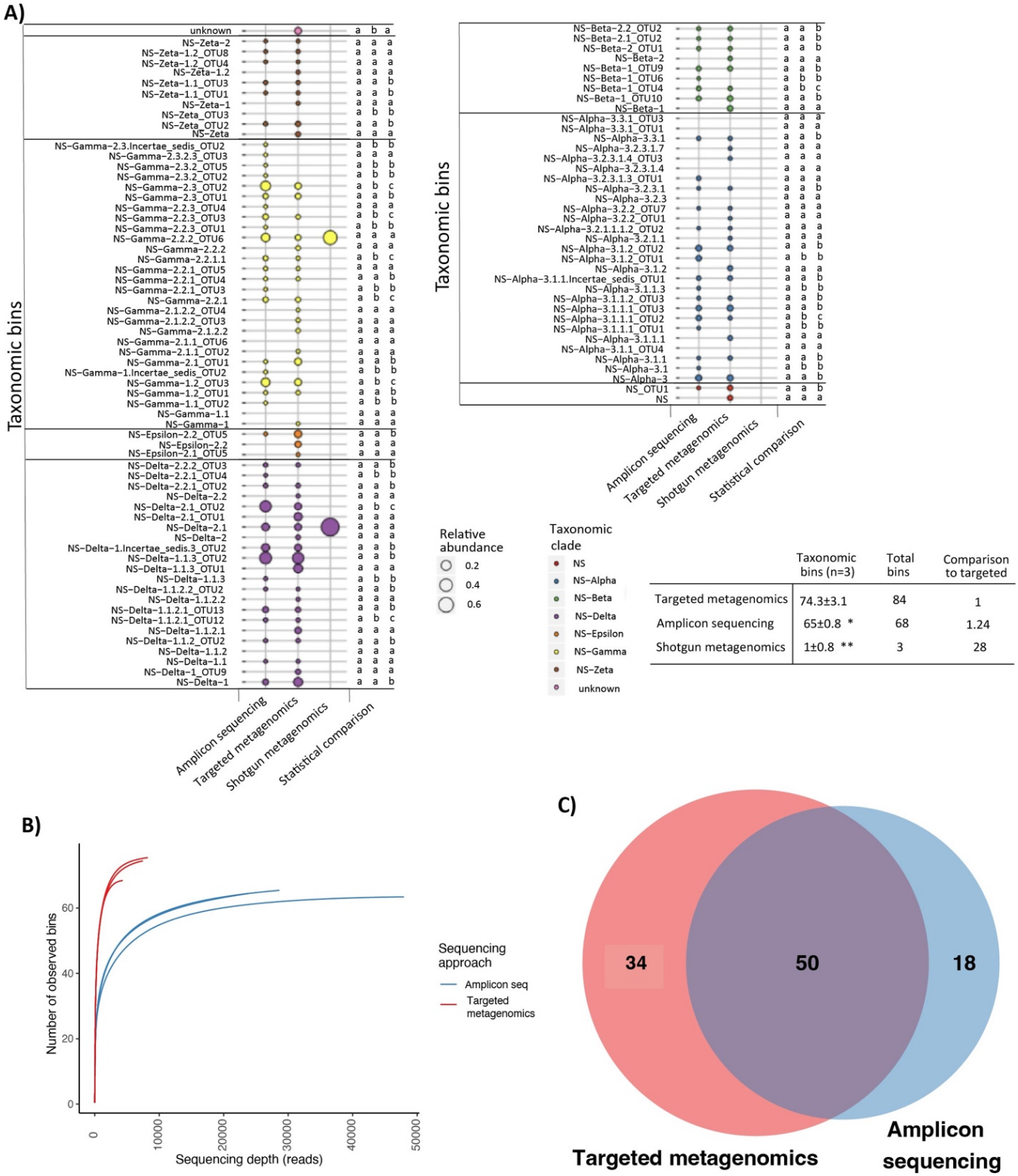

	Taxonomic bins (n=3)	Total bins	Comparison to targeted
Targeted metagenomics	74.3±3.1	84	1
Amplicon sequencing	65±0.8 *	68	1.24
Shotgun metagenomics	1±0.8 **	3	28

1136
1137 Fig. 4. A) The relative abundance of archaeal *amoA* taxonomic bins produced from amplicon
1138 sequencing with *amoA* amplicon sequencing (*amoA* gene PCR amplicons sequenced with Illumina
1139 MiSeq, about 22000-47000 *amoA* reads per sample) (n = 3), metagenomics reads of targeted
1140 metagenomics (genomic DNA sequenced with Illumina MiSeq, after target enrichment, about
1141 4500-8500 *amoA* reads out of 220000-310000 targeted reads per sample)(n = 3), or shotgun
1142 metagenomics (genomic DNA sequenced with Illumina HiSeq, about 22-57 million reads per
1143 sample, of which only two were archaeal *amoA*)(n = 3). In all cases, the analysis pipeline consisted
1144 of USEARCH comparison on *amoA* reference database (Alves et al., 2018) and taxonomy were
1145 analyzed with QIIME1 analytical pipeline. Sample having largest diversity is shown (n = 3).
1146 Bubble symbol size is proportional to the relative abundance of each taxonomic bin produced with
1147 sequencing approach in each sequencing method. Color indicates Nitrosospheria (NS)-clade of
1148 taxonomic bin. Statistically significant differences in abundance of each taxonomic bins between
1149 sequencing approaches based on Pairwise-Wilcox comparison are indicated with different letters
1150 ($P < 0.05$, n=3), and the significant difference of comparison for taxonomic bins is shown an
1151 asterisk, * $P<0.05$, ** $P<0.01$. B) The rarefaction analysis of archaeal *amoA* obtained by amplicon
1152 sequencing and captured metagenomics. C) Venn-diagram of archaeal *amoA* sequences obtained
1153 by amplicon sequencing and targeted metagenomics.
1154

1155